Bioorganic Chemistry 88 (2019) 102973

Contents lists available at ScienceDirect

Bioorganic Chemistry

journal homepage: www.elsevier.com/locate/bioorg

Identification of anti-inflammatory polyketides from the coral-derived fungus *Penicillium sclerotiorin*: *In vitro* approaches and molecular-modeling

Zhaoming Liu[a,b,1], Pei Qiu[a,1], Hongju Liu[c], Jing Li[c], Changlun Shao[d,*], Tao Yan[e], Wenhao Cao[e], Zhigang She[a,*]

[a] School of Chemistry, Sun Yat-Sen University, Guangzhou 510275, PR China
[b] State Key Laboratory of Applied Microbiology Southern China, Guangdong Provincial Key Laboratory of Microbial Culture Collection and Application, Guangdong Open Laboratory of Applied Microbiology, Guangdong Institute of Microbiology, 100 Central Xianlie Road, Yuexiu District, Guangzhou 510070, PR China
[c] School of Pharmacy, Guangdong Medical University, Dongguan 523808, PR China
[d] Key Laboratory of Marine Drugs, The Ministry of Education of China, School of Medicine and Pharmacy, Ocean University of China, Qingdao 266003, PR China
[e] CAS Key Laboratory of Tropical Marine Bio-resources and Ecology, Guangdong Key Laboratory of Marine Materia Medica, RNAM Center for Marine Microbiology, South China Sea Institute of Oceanology, Chinese Academy of Sciences, 164 West Xingang Road, Guangzhou 510301, PR China

ARTICLE INFO

Keywords:
Polyketides
Azaphilones
Gorgonian-derived fungus
Anti-inflammatory

ABSTRACT

Four new polyketides, including an unusual naphthoquinone derivative (**1**), two azaphilone analogous (**2**, **7**) and an α-pyrone (**12**), were isolated from the gorgonian-derived fungus *Penicillium sclerotiorum* CHNSCLM-0013 together with nine known compounds. Their structures were identified based on the 1D, 2D NMR, HRESIMS, single crystal X-ray diffraction and the absolute configurations were determined by comparing the ^{1}H NMR chemical shift and optical rotations with those reported in literature. In the bioassay, compounds **2**, **6**, **7**, **10** and **12** exhibited significant inhibitory activities against the nitric oxide (NO) production in the LPS-induced macrophage RAW 264.7 with the IC_{50} values in the range of 2.5–18.0 μM. Compounds **2**, **6** and **7** exhibited the possible mechanism of downregulating the expression of iNOS and COX-2 in mRNA level. The primary structure-activity relationship was also discussed based on the molecular-modeling. This study will make a contribution to the chemical diversities of polyketides especially the azaphilone derivatives and the discovery of potential anti-inflammatory agent from marine fungi.

1. Introduction

Marine ecosystem has become a “huge treasury” of new bioactive natural products (NPs), which refers to naturally occurring small secondary metabolites (usually < 3000 Daltons) from marine environment or organisms such as molluscs and microorganisms [1–3]. These NPs make significant contributions not only to organism’s survival, growing or biophylaxis, but also to the increasing number of therapeutic agents being developed in preclinical researches or clinical applications for life sciences [4,5].

Marine microorganisms, play as the most important source of natural products from marine ecosystem, have generated considerable interest in the past decades. The extreme environment promotes the production of metabolites with interesting skeleton and potent bioactivities, such as the *Mycobacterium tuberculosis* protein tyrosine phosphatase B (MptpB) inhibitor asperterpenoid A [6], diaporisoindole A [7]; COX-2 expression inhibitor dysiarenone [8] and influenza neuraminidase agent simpterpenoid A [9]. By 2016, the number of new metabolites from marine microorganisms has reached half of the total number of marine natural products [1–3]. On our ongoing search for structural unique and biological active metabolites from marine microorganisms [6,7,10–12], the chemical investigation of a gorgonian-derived fungus Penicillium sclerotiorum CHNSCLM-0013 was carried out and four new polyketides including an unusual naphthoquinone derivative (**1**), two azaphilone analogous (**2**, **7**) and an α-pyrone (**12**), were obtained based on ^{1}H NMR spectroscopy-guided strategy together with nine known compounds. Moreover, compounds **2**, **6**, **7**, **10** and **12** exhibited significant inhibitory activities against the nitric oxide (NO) production in the LPS-induced macrophage RAW 264.7 with the IC_{50} values in the range of 2.5–18.0 μM. Herein, the details of the isolation, structure identification and biological activities assays were discussed.

* Corresponding authors.
E-mail address: cesshzhg@mail.sysu.edu.cn (Z. She).
[1] Z. Liu and P. Qiu contributed equally.

https://doi.org/10.1016/j.bioorg.2019.102973
Received 22 March 2019; Received in revised form 30 April 2019; Accepted 3 May 2019
Available online 04 May 2019
0045-2068/

2. Material and methods

2.1. General experimental procedures

UV data were collected on a UV-240 spectrophotometer (Shimadzu, Beijing, China). IR spectrum was recorded using Bruker Vector spectrophotometer 22. Melting points were tested on a Fisher-Johns hot-stage apparatus and were uncorrected. Optical rotation was recorded using a MCP300 (Anton Paar, Shanghai, China). HRESIMS were determined with a Q-TOF high-resolution mass spectrometer (Waters). The experiment ECD data were recorded on J-810 spectropolarimeter (JASCO, Tokyo, Japan). 1D and 2D NMR data were recorded on a Bruker Avance spectrometer (Bruker, Beijing, China), in which all chemical shifts (δ) are given in ppm with reference to TMS and coupling constants (J) are given in Hz. Column chromatography (CC) was carried out on silica gel (200–300 mesh, Marine Chemical Factory, Qingdao, China) and sephadex LH-20 (Amersham Pharmacia, Piscataway, NJ, USA). Solvents used to column chromatography were analytically pure with prior distilled to remove the water and the high boiling point impurities. Semipreparative HPLC was performed on a Waters Breeze HPLC system using a Phenomenex Luna (Phenomenex, Torrance, CA, USA) C18 column (250 × 10 mm, 5 μm), flow rate, 2.0 mL/min. The measurement of the absorbance in anti-inflammatory activity was performed with an Infinite M200 PRO microplate reader (TECAN). RT-PCR amplification was carried out using PikoReal (Thermo Fisher Scientific, MA, USA).

2.2. Fungal material

The fungus strain *Penicillium sclerotiorum* used in this study was isolated from a piece of fresh tissue of the inner part of the gorgonian coral *A. ocbracea* (GXWZ-33), which were collected in April 2010 from Weizhou coral reef in South China Sea. It was obtained using the standard protocol for the isolation. Fungal identification was carried out using a molecular biological protocol by DNA amplification and sequencing of the ITS region of the rRNA gene. The 543 based pair ITS sequence data obtained from the fungal strain have been deposited at GenBank with accession no. KT695601. A BLAST search result showed that the sequence was the most similar (99%) to the sequence of *P. sclerotiorum* (compared to KF999008.1). The strain was deposited at the Key Laboratory of Marine Drugs, the Ministry of Education of China, Qingdao, PR China.

2.3. Fermentation, extraction and isolation

The fungus was grown on solid cultured medium in 60 Erlenmeyer flasks (each containing 100 g rice and 150 mL 0.3% saline) for 28 days at room temperature under static condition. After fermentation, the former was extracted with Methanol for three times and then concentrated under reduced pressure to yield residual gum in 35.4 g. The extract was subjected to silica gel CC using gradient elution with petroleum ether-Ethyl acetate from 90:10 to 0:100 (v/v) to give 36 fractions (Frs.1–30). Fr. 5 (9.8 g) was recrystallized to offer **3** (1.5 g). Fr. 14 (2.0 g) was further subjected to silica gel CC using dichloromethane/methanol (98:2) to obtain Fr.14.1–14.10. Fr. 14.2 (321.2 mg) was purified by Sephedx LH-20 CC eluted with methanol/dichloromethane (1/1) to obtain **1** (2.8 mg), **2** (2.5 mg), **7** (3.7 mg), **8** (7.1 mg). Fr. 14.5 (305.9 mg) was subjected to silica gel using chloroform/methanol (98:2) and semi-preparation HPLC to afford **9** (2.3 mg), **10** (3.9 mg) and **11** (4.4 mg). Fr. 25 (999.0 mg) was applied to repeated Sephedx LH-20 CC where 4 (9.8 mg), 5 (11.6 mg) and **6** (39.8 mg) were obtained. Finally, **12** (2.2 mg) and **13** (6.5 mg) were isolated in the Fr. 27 using semi-preparation HPLC.

2.3.1. Sclerketide A (1)

Yellow crystal; *m.p.* 234–235 °C; [α] + 89.2 (c 0.01, $CHCl_3$); UV (MeOH) λ_{max} (logε): 248 (4.88), 257 (3.81), 309 (3.41), 352 (3.26) nm. IR (KBr): 3326, 2851, 2713, 1690, 1680, 1675, 1298, 1011, 904 cm^{-1}; HRESIMS *m/z* 353.1397 $[M–H]^-$ (calcd for $C_{21}H_{21}O_5$, 353.1384); ^1H and ^{13}C NMR data: see Table 1.

Table 1
^1H (500 MHz) and ^{13}C (125 MHz) NMR Data of **1** and **2**.

Position	**1**[a]		Position	**2**[a]	
	δ_H (mult, *J*, Hz)	δ_C		δ_H (mult, *J*, Hz)	δ_C
1		180.4 C	1	7.94 (s)	152.6 CH
2		153.5 C	2		
3		121.9 C	3		157.8 C
4		183.7 C	4	6.65 (s)	106.3 CH
4a		134.4 C	4a		138.6 C
5	7.64 (s)	116.5 CH	5		110.8 C
6		166.5 C	6		185.9 C
7		123.2 C	7		84.4 C
8	8.64 (s)	129.3 CH	8		191.9C
8a		123.7 C	8a		114.4 C
9	2.14 (s)	8.9 CH_3	9	6.08 (d, 15.7)	115.6 CH
10		193.9 C	10	7.06 (d, 15.7)	142.8 CH
11	7.09 (d, 15.0)	116.9 CH	11		132.0 C
12	7.68 (d, 15.0)	153.5 CH	12	5.71 (d, 9.8)	148.8 CH
13		132.4 C	13	2.49 (m)	35.2 CH
14	5.99 (d, 9.8)	154.1 CH	14	1.43 (m)	30.1 CH_2
15	2.55 (m)	34.5 CH		1.33 (m)	
16	1.46 (m)	29.9 CH_2	15	0.87 (t, 7.4)	11.8 CH_3
	1.37 (m)		16	1.85 (s)	12.3 CH_3
17	0.89 (t, 7.5)	11.9 CH_3	17	1.01 (d, 6.5)	20.2 CH_3
18	1.97 (s)	12.7 CH_3	18	1.57 (s)	22.5 CH_3
19	1.05 (d, 6.6)	20.0 CH_3	1′		173.8 C
6-OH	13.04 (s)		2′	2.49 (q, 7.5)	26.6 CH_2
			3′	1.15 (t, 7.5)	8.72 CH_3

[a] Measured in chloroform-*d*.

2.3.2. Sclerketide B (2)

Yellow power; *m.p.* [α] = + 406 (c 0.1, methanol); UV (MeOH) λ_{max} (logε): 240 (4.51), 288 (3.93), 332 (1.23) nm. IR (KBr): 3435, 2949, 1737, 1625, 1512, 1183, 1131, 1079, 966 cm^{-1}; HRESIMS *m/z* 405.1465 ($[M+H]^+$) (calcd for $C_{22}H_{26}O_5Cl$, 405.1463); ^1H and ^{13}C NMR data: see Table 1.

2.3.3. Sclerketide C (7)

Yed oil; [α] = + 399 (c 0.1, methanol); UV (MeOH) λ_{max} (logε): 24 (3.32), 376 (3.28), 480 (3.01) nm. IR (KBr): 2950, 2920, 1740, 1709, 1600, 1491, 1222, 1150, 853 cm^{-1}; HRESIMS *m/z* 490.1991 ($[M+H]^+$, calcd for $C_{26}H_{33}O_6NCl$, 490.1991); ^1H and ^{13}C NMR data: see Table 1.

2.3.4. Sclerketide D (12)

Yellowish power; [α] = + 39 (c 0.1, methanol); UV (MeOH) λ_{max}: 222 (3.33), 254 (2.99) nm. IR (KBr): 3316, 2933, 1634, 1414, 1309, 1135 cm^{-1}; HRESIMS *m/z* 309.1708 ($[M–H]^-$, calcd for $C_{21}H_{21}O_6$, 309.1707; ^1H and ^{13}C NMR data: see Table 2.

2.4. Crystallographic data and X-ray analysis

Data were collected on an Agilent Xcalibur Nova single-crystal diffractometer using Cu Kα radiation. The crystal structure was refined by full-matrix least-squares calculation with the SHELXL-97. Crystallographic data for the structure of **1** have been deposited in the Cambridge Crystallographic Data Centre (deposition number: CCDC 1826093). Crystal data of **1**: $C_{21}H_{22}O_5$ (M = 254.38); needle crystal (0.05 × 0.11 × 0.2); space group *P*1; unit cell dimensions a = 6.1358(2) Å, b = 11.0077(5) Å, c = 13.3588(6) Å, α = 91.540(4)°, β = 100.013(3)°, γ = 91.645(3)°, V = 887.69(6) $Å^3$, Z = 2; T = 150(2) K; ρ_{cald} = 1.326 mg/m^3; absorption coefficient 0.771 mm^{-1}; F (000) = 376, a total of 7741 reflections were collected in the range

Table 2
^{1}H (500 MHz) and ^{13}C (125 MHz) NMR Data of **7** and **12**.

	7[a]			**12**[a]	
Position	δ_H (mult, J[b])	δ_C	Position	δ_H (mult, J[b])	δ_C
1	7.74 (s)	141.1 CH	1		168.1 C
2			2		97.2 C
3		148.1 C	3		168.6 C
4	7.04 (s)	111.4 CH	4	6.02 (s)	102.9 CH
4a		144.5 C	5		160.3 C
5		114.8 C	6	2.50 (dd, 14.5, 8.2)	41.2 CH_2
6		184.5 C		2.62 (dd, 14.5, 4.7)	
7		84.8 C	7	3.90 (m)	68.5 CH
8		194.0 C	8	1.57 (m)	35.2 CH_2
8a		102.3 C	9	2.07 (ddd, 14.4, 9.4, 6.1)	35.2 CH_2
9	6.30 (d, 15.3)	114.6 CH		2.17 (ddd, 14.4, 9.5, 5.8)	
10	7.00 (d, 15.3)	145.4 CH	10		134.3 C
11		132.1 C	11	5.02 (d, 9.7)	128.3 CH
12	5.71 (d, 9.7)	148.2 CH	12	2.33 (m)	40.0 CH
13	2.48 (m)	35.2 CH	13	3.45 (m)	71.7 CH
14	1.44 (m)	30.1 CH_2	14	1.10 (d, 6.3)	20.3 CH_3
	1.35 (m)		15	1.85 (s)	7.2 CH_3
15	0.88 (t, 7.4)	12.6 CH_3	16	1.65 (s)	15.1 CH_3
16	1.90 (s)	12.1 CH_3	17	0.96 (d, 6.7)	16.3 CH_3
17	1.02 (d, 6.7)	20.3 CH_3			
18	1.55 (s)	23.3 CH_3			
1′	3.74 (m)	53.0 CH_2			
2′	2.06 (m)	25.3 CH_2			
3′	2.44 (br t, 6.5)	30.0 CH_2			
4′		172.4 C			
OMe	3.70 (s)	52.2 CH_3			

[a] Measured in chloroform-*d*.
[b] J in Hz.

8.04° < θ < 73.52°, independent reflections 3996 [R(int) = 0.0369]; the number of data/parameters/restraints were 3996/3/484; goodness-of fit on F^2 = 1.054; final R indices [$I > 2\sigma(I)$] R_1 = 0.0467, ωR_2 = 0.1249; R indices (all data) R_1 = 0.0522, ωR_2 = 0.1281.

2.5. The Anti-inflammatory activity

The anti-inflammatory activities of isolated metabolites were evaluated on the basis of the inhibition of NO production in lipopolysaccharide (LPS)-induced RAW 246.7 mouse macrophages according to the reported methods. The cytotoxicity against the macrophages were assayed using the MTT method. RAW 264.7 cells used in this study were purchased from the cell bank of the Chinese Academy of Sciences from Shanghai. Firstly, the cells were cultured in 96-well plates at a density of 0.00005 cells per well and incubated overnight (12 h). Then, LPS with concentration of 1 μg/mL was added together with the different concentrations of tested compounds (dissolved in dimethyl sulphoxide). After 24 h, 50 μL cell culture supernatant solution was moved to a new plate which contained NO detection reagent I (50 μL) and II (50 μL). Finally, the absorbance was measured at 540 nm.

2.6. Reverse transcriptase-PCR (RT-PCR)

Total RNA was extracted from RAW264.7 cells using Trizol reagent. The primers (Generay, guangzhou, China) were described as following: mouse iNOS (129 bp), forward primer 5′-CTTGGAGCGAGTTGTGGATT GTC-3′ and reverse primer 5′-TAGGTGAGGGCTTGGCTGAGTG-3′; mouse COX-2 (166 bp), forward primer 5′-TAGTTGCTCATCACCCCA CTC-3′ and reverse primer 5′-GATCTACCCTCCTCACATCCC-3′;PCR was performed over 35 cycles of denaturation at 95 °C for 5 min, annealing at 57 °C for 15 s, and elongation at 72 °C for 20 s. Aliquots (6 μL) were electrophoresed in 1.2% agarose gels and stained with ethidium bromide [13].

2.7. Molecular docking study

Tested compounds were optimized using DFT calculations at the B3LYP/6-31G(d) level through the Gaussian 09 program [14]. Docking simulations in iNOS were carried out in AutoDock4.2.6 [15]. The crystallographic structure of iNOS was downloaded from the Protein Data Bank (pdb code: 2BHJ). The method used was according to the previously reported [16]. The energy grid maps for each atom type in the ligands (i.e. A, C, HD, N, and OA), as well as the electrostatic and de-solvation maps were calculated using the AutoGrid 4.2.6 program. The optimal binding conformation was determined by LGALS (Lamarckian Genetic Algorithm with Local Search) with the same parameters as previously reported during each run. Docking runs were carried out and the resulting 100 binding conformations were generated according to the calculated binding free energy. The obtained results and the docked poses were analyzed by AutoDockTools.

3. Results and discussion

3.1. Metabolites isolation

The methanol extract of the fermentation broth was subjected to repeated silica gel, Sephadex LH-20 column chromatography and reversed-phase C_{18} semipreparative High Performance Liquid Chromatography (HPLC) to afford 15 fractions. ^{1}H NMR (500 MHz) spectra of each fraction were acquired in dimethyl sulphoxide with a concentration of 1 mg/mL and most of them displayed signals of a 2-butyl moiety: δ_H 2.45–2.55 (m, CH); δ_H 1.31–1.39, 1.40–1.48 (each m, CH_2); δ_H 1.00–1.05 (d, J = 6.5, CH_3); δ_H 0.85–0.90 (t, J = 7.5, CH_3), which were well known to occur within the side chain of azaphilones. Guided by the characteristic resonances, thirteen relative polyketides (**1**–**12**) including an unusual naphthoquinone derivative sclerketide A (**1**), two new azaphilone analogous sclerketide B–C (**2**, **7**) and a new α-pyrone derivative sclerketide D (**12**) were obtained (Fig. 1). The structures of the new compounds were deduced based on the 1D, 2D NMR spectroscopic data, X-ray diffractions and optical rotations (Fig. 1). The known compounds were identified as (+)-sclerotiorin (**3**), deacelysclerotioramine (**4**), isochromophilone VI (**5**), isochromophilone IX (**6**), isochromophilone IV (**8**), ochlephilone (**9**), sequoiatones B (**10**), sequoiatones A (**11**), and 6-((1E,3E)-3,5-dimethylhepta-1,3-dien-1-yl)-2,4-dihydroxy-3-methylbenzaldehyde (**13**) by comparing their spectroscopic data with those reported [17–23].

3.2. Structure identification

Sclerketide A (**1**) was obtained as flavescent crystals. The molecular formula was deduced to be $C_{21}H_{22}O_5$ based on the HRESIMS at quasi-molecular ion peaks m/z 353.1397 $[M–H]^-$ (calcd for $C_{21}H_{21}O_5$, 353.1384), suggesting 11 degrees of unsaturation. ^{1}H NMR spectrum (Table 1) displayed signals of a chelating proton at δ_H 13.04 (s, 6-OH); three olefinic protons including a set of trans coupled ones at δ_H 7.09 (d, J = 15.0 Hz, H-11), 7.68 (d, J = 15.0 Hz, H-12); two singlet aromatic protons at δ_H 7.64 (s, H-5), 8.64 (s, H-8); two singlet methyl signals at δ_H 2.14 (s, H_3-9); δ_H 1.97 (s, H_3-18) and a 2-butyl resonance at δ_H 0.89 (t, J = 7.5 Hz, H_3-17), δ_H 1.05 (d, J = 6.6 Hz, H_3-19), δ_H 2.55 (m, H-15); δ_H 1.37, 1.46 (each m, H_2-16). ^{13}C NMR data indicated the presences of 21 carbons including 12 aromatic carbons and three carbonyl carbons. Further analysis of the ^{1}H, ^{1}H-COSY spectrum (Fig. 2) suggested that there were two independent spin-coupling systems (C-11–C-12 and C-14–C-17) based on the correlations of H-11/H-12 and H-14/H-15(H-19)/H_2-16/H_3-17.

The planar structure was determined by HMBC analysis (Fig. 2). The correlations from H-8 to C-7/C-1/C-8a, H-5 to C-3/C-4a/C-8a and the labile proton 6-OH to C-5/C-6/C-7 suggested the naphthoquinone

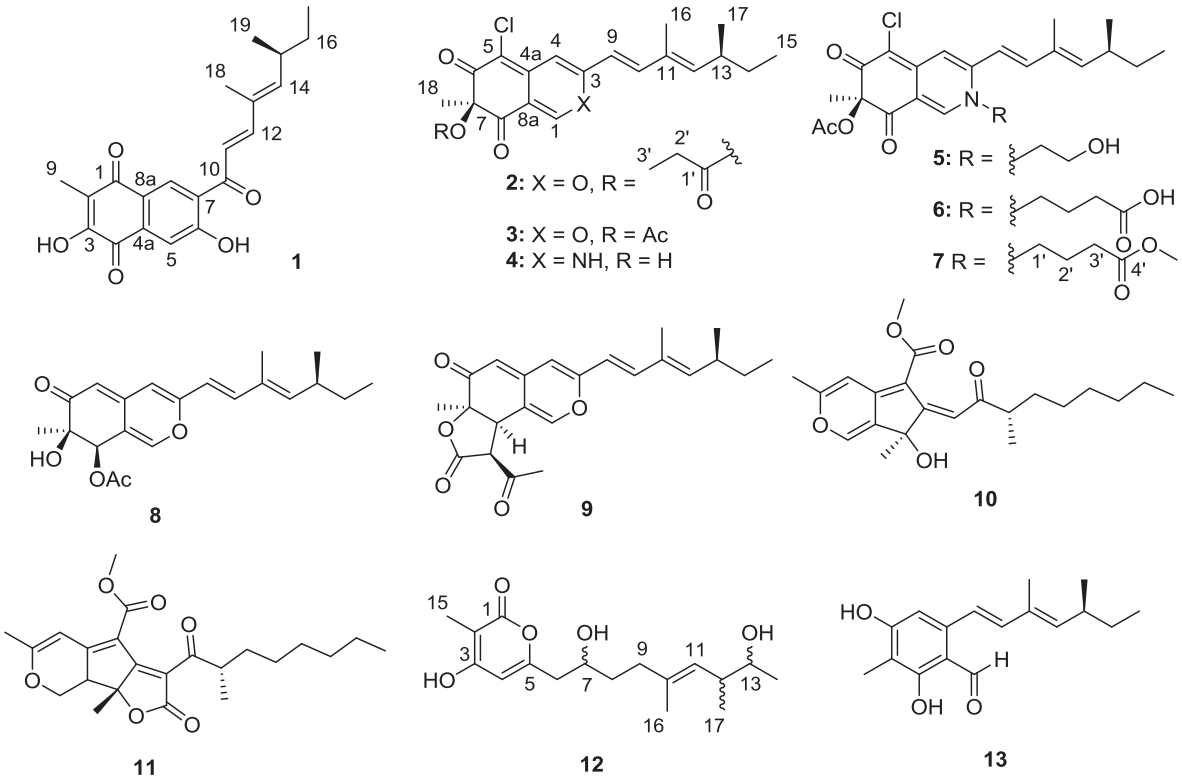

Fig. 1. Chemical structures of compounds **1**–**13**.

skeleton. The connectivity of the two spin-coupling systems was deduced by the cross-peak from H_3-18 to C-12, C-13 and C-14, which formed the characteristic side chain. Furthermore, based on the correlations from H-8 to C-10, C-11 and C-12, the linkage of the naphthoquinone moiety and the side chain was constructed via the carbonyl carbon (C-10). Finally, the methyl H_3-9 was linked to C-2 which was evidenced by the correlations from H_3-9 to C-1, C-2 and C-3.

The block crystal of **1** was obtained in the mix solvent of methanol/$CHCl_3$ (1/15) and the geometry of $\triangle_{13,14}$ was further confirmed by the X-ray diffractions (Fig. 3). The absolute configuration of C-15 was proposed to be *S* by comparing the characteristic ^1H and ^{13}C chemical shifts of CH-15, Me-19 and CH_2-16 with those reported azaphilones which contained a same side chain (C-10–C-19) [17,18,24].

Sclerketide B (**2**) was isolated as yellowish oil. Analysis of the HRESIMS afforded a deprotonated molecular peak at *m/z* 405.1465 ([M + H]$^+$), suggesting the molecular formula to be $C_{22}H_{26}O_5Cl$ (calcd for $C_{20}H_{22}O_5Cl$, 405.1463). ^1H and ^{13}C NMR spectrum revealed the presences of five substituted double bonds, two keto groups, four methyls, one methane and a methine (Table 1), indicating that compound **2** was an azaphilone derivative similar to (+)-sclerotiorin (**3**). The main difference is that the acetyl was absence in (+)-sclerotiorin (**3**) and an

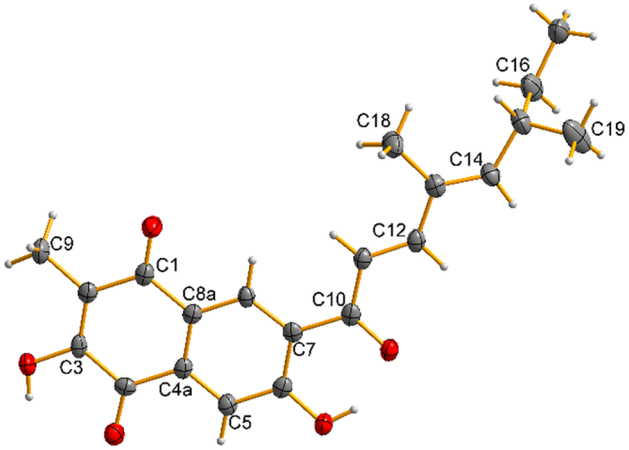

Fig. 3. The crystal structure of compounds **1**.

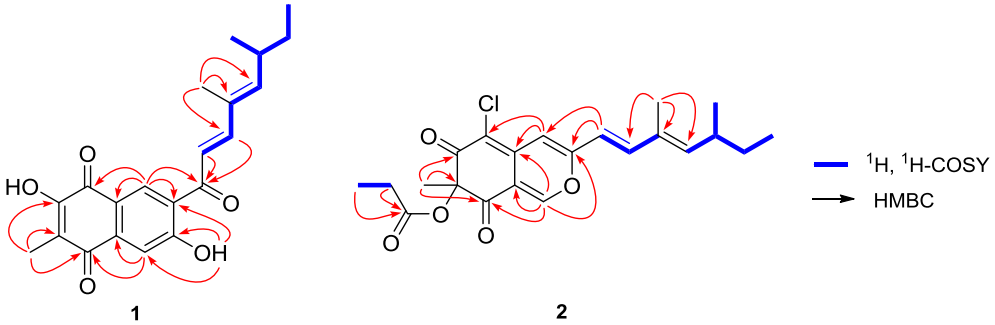

Fig. 2. ^1H, ^1H-COSY and HMBC correlations of compounds **1** and **2**.

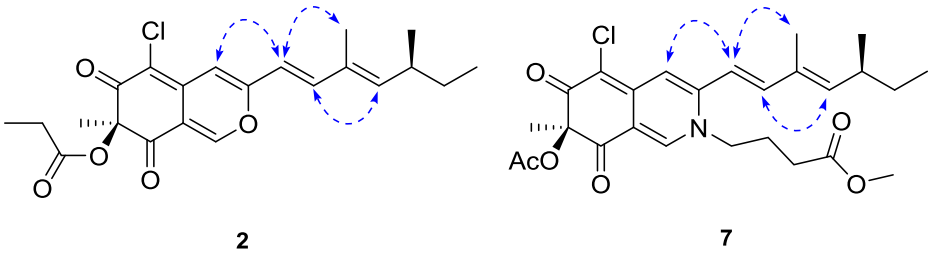

Fig. 4. NOESY correlations of compounds **2** and **7**.

additional propionyl group was appeared [δ_H 2.49 (q, J = 7.5 Hz), δ_H 1.15 (t, J = 7.5 Hz), δ_C 173.8]. Considering about the chemical shift of C-7 (δ_C 84.4), the propionyl group should be connected to C-7.

The geometry of double bonds $\triangle^{9,10}$ and $\triangle^{11,12}$ were deduced based on the coupling constants of H-10 and H-11 (J = 15.7 Hz) as well as the NOE correlation of H_3-16/H-9 and H-10/H-12 (Fig. 4). Furthermore, the absolute configuration of C-7 was determined as *R* based on the positive optical rotation [+406 (c 0.1, methanol)]. The chirality of C-13 of the side chain was signed as *S* by comparison the NMR data with the known relatives (+)-sclerotiorin [17,24].

Sclerketide C (**7**) was isolated as red oil, of which the molecular formula was determined to be $C_{26}H_{32}O_6NCl$ based on the quasi-molecular ion peak m/z 490.1991 ($[M+H]^+$, calcd for $C_{26}H_{33}O_6NCl$, 490.1991) from HRESIMS. Comprehensive analysis of the ^1H and ^{13}C NMR (Table 2) data indicated that compound **7** also constructed an azaphilone skeleton containing a nitrogen atom. Comparing to the previously reported metabolite isochromophilone IX (**6**) from *Penicillium* sp. suggested that an additional methoxyl was present. The HMBC correlation (Fig. 5) from Me-5′ to the neighboring carbonyl carbon C-4′ confirmed the methylation of the carboxyl (C-4′). The absolute configuration of C-7 was determined as *R* based on the positive optical rotation [+399 (c 0.1, methonal)] and the geometry of $\triangle^{9,10}$ and $\triangle^{11,12}$ were established by the coupling constants and NOE correlations (Fig. 4), respectively [21]. Hence, compound 7 was established to be methyl ester of isochromophilone IX, named sclerketide C.

Sclerketide D (**12**) was obtained as colorless power and its molecular formula was deduced as $C_{17}H_{26}O_5$ based on the HRESIMS (m/z 309.1708 ($[M-H]^-$, calcd for $C_{21}H_{21}O_6$, 309.1707). ^1H NMR data indicated the presences of two tri-substituted olefin protons (δ_H 6.02 (s), 5.02 (d, J = 9.7)), three methenes including two with AB coupling system (δ_H 2.50 (dd, J = 14.5, 8.2), 2.62 (dd, J = 14.5, 4.7); δ_H 2.07 (ddd, J = 14.4, 9.4, 6.1), 2.17 (ddd, J = 14.4, 9.5, 5.8)), two oxygen bearing methines (δ_H 3.90 (m), 3.45 (m)) and four methyl groups (δ_H 0.96, 1.10, 1.65, 1.85). ^{13}C NMR revealed the containment of four aromatic carbons, ten sp3 hybridized carbons and an α, β-unsaturated carbonyl carbon (δ_C 168.1).

Furhter analysis of the 2D NMR spectrum (Fig. 6) constructed the gross structure. The correlations of H_2-6/H-7/H_2-8/H_2-9 and H-11/H-12(H_3-17)/H-13/H_3-14 in ^1H, ^1H-COSY spectrum suggested that there were two independent spin coupling system (C-5–C-9 and C-11–C-14, respectively). The α-pyrone was elucidated based on the HMBC correlations from Me-15 to C-1/C-2/C-3, H-4 to C-3/C-4/C-5 as well as the requirement of degrees of unsaturation. The cross peaks from H_2-6 to C-4/C-5 indicated the linkage between C-5 and C-6 and the two spin

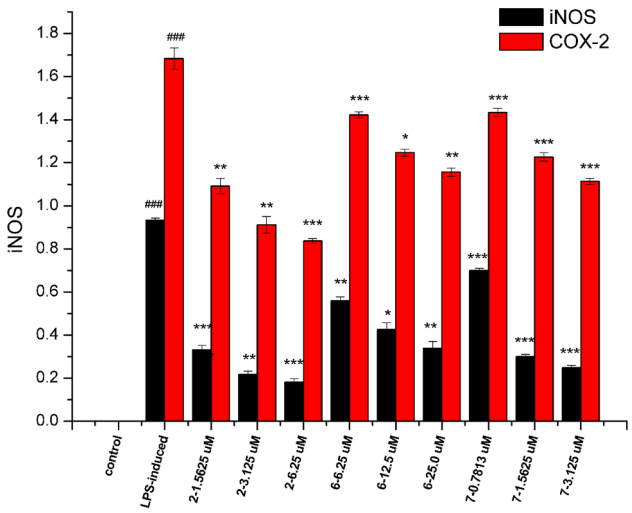

Fig. 6. Effect of **2**, **6** and **7** on the relative mRNA expression levels of iNOS and COX-2 in LPS-activated RAW 264.7 cells. RAW 264.7 cells were pretreated with different concentrations of tested compounds for 30 min, followed by LPS treatment for 24 h. RNA was extracted and used in the qRT-PCR reaction. $^{###}p < 0.001$ vs untreated controls. $^{*}p < 0.05$, $^{**}p < 0.01$ and $^{***}p < 0.001$ vs LPS treated cells.

moieties were connected through $\Delta^{10,11}$ evidenced by the correlations from Me-16 to C-9, C-10 and C-11. Hence, the planar structure was established as shown. However, due to the limited quantity, using modified method to establish the absolute configuration was failed and the stereo chemistry was still unknown.

3.3. Proposed biosynthesis pathway

The proposed biosynthesis pathway of the new metabolites was performed in Scheme 1. Firstly, the 3,5-dimethyloctadienone moiety was formed by three molecules of malonyl-CoA and two molecular SAMs (S-adenosyl methionines) based on the HR-PKS. Then, five additional malonyl-CoAs were loaded and the following aldol condensation constructed a naphthalene nucleus, which further formed sclerketide A (**1**). Meanwhile, the azaphilone and the α-pyrone moiety could be generated by 4 Mal-CoAs/1 SMA or 3 Mal-CoAs/1 SMA, respectively, following by the reduction, esterification and condensation to yield **2**, **7** and **12** [25,26].

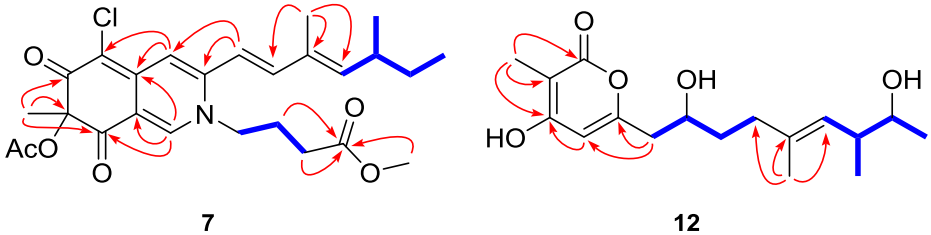

Fig. 5. ^1H, ^1H-COSY and HMBC correlations of compounds **7** and **12**.

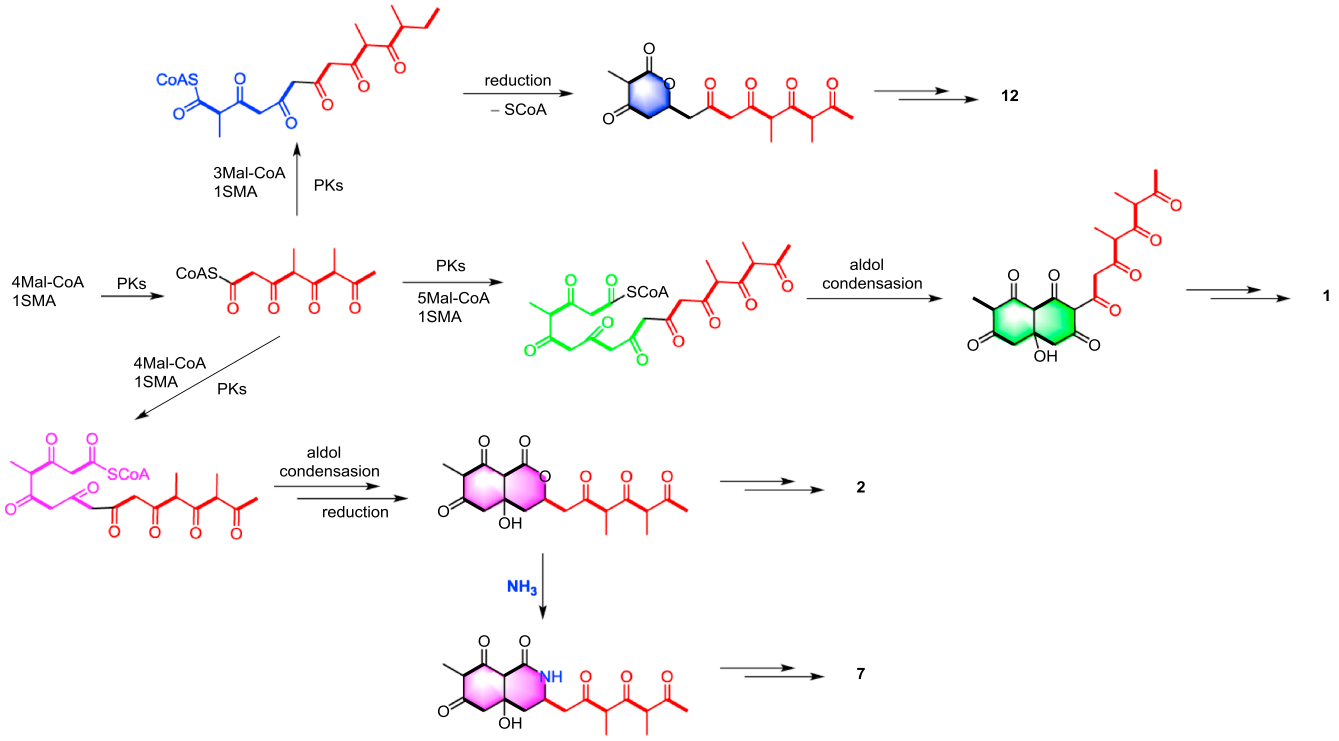

Scheme 1. The proposed biosynthesis pathway of the new compounds.

3.4. Inhibitory effects of NO production

The anti-inflammatory activities of the isolated metabolites were evaluated on the basis of their inhibition effects of NO production in the lipopolysaccharide (LPS)-induced mouse macrophages. The summarized results were presented in Table 3. Compounds **2**, **6**, **7**, **10** and **12** exhibited potential inhibitory effect against the production of NO with the IC_{50} values in the range of 2.5–18.0 μM, of which sclerketide C (**7**) was the most active (IC_{50} = 2.7 μM). However, it also showed moderate cytotoxicity with the IC_{50} values of 14.8 μM (Selective Index = 5.48). The structure-activity analysis between **6** and **7** indicated that the terminal methoxy group made a significant contribution to the anti-inflammatory effect as well as the cytotoxicity. In order to investigate the possible mechanism of inhibiting NO production, the mRNA levels of iNOS and COX-2 in LPS-induced RAW 264.7 were measured by reverse transcriptase-PCR (RT-PCR). Besed on the IC_{50} values, three different concentrations were selected and the results were shown in Fig. 6. Although both compounds **2**, **6** and **7** could suppress the mRNA expression of iNOS and COX-2 in LPS-induced RAW 264.7 in a concentration dependent way, greater effects were observed against iNOS and compound **7** exhibited most significant inhibitory activity compared with the other compounds.

Table 3
Results of anti-inflammatory activity and cytotoxicity.

	Inhibition of NO production (IC_{50}/μM)	Cytotoxicity (IC_{50}/μM)	SI[b]
2	3.4 ± 0.5	> 200	–
6	17.6 ± 0.7	> 200	–
7	2.7 ± 0.5	14.8 ± 1.0[c]	5.48
10	5.2 ± 0.6	> 200	–
12	5.5 ± 0.5	> 200	–
Indomethacin[a]	30.7 ± 0.9	> 200	–

[a] Positive control.
[b] Selective index.
[c] Inhibitory rate of 13% at 2.7 μM.

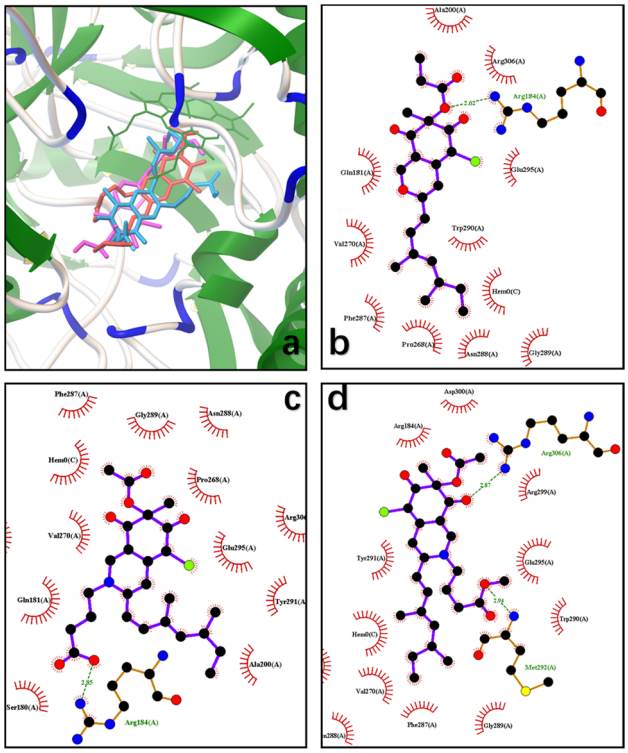

Fig. 7. The molecular-modeling of compounds **2**, **6** and **7**.

3.5. Inhibitory effects of NO production

Next, the simulative molecular-docking analyses of compounds **2**, **6** and **7** with iNOS were performed to gain insight interaction between inhibitors and protein (Fig. 7). Both of them binded in the same catalytic site of iNOS with binding energy of −9.43, −9.33 and −10.49 kcal/mol, respectively. Notably, compounds **2** and **7** had a

similar binding pose while **6** exhibited an opposite orientation in the pocket. Hydrogen bond between inhibitors and guanidine group of Arg184 or Arg306 was proposed to make the key contribution to the inhibitory activities. The above findings suggested that these compounds could be further developed as anti-inflammatory therapeutic lead compounds.

4. Conclusions

In conclusion, four new polyketides, including an unusual naphthoquinone derivative (**1**), two azaphilone analogous (**2**, **7**) and an α-pyrone (**12**), as well as nine known compounds (**3–6**, **8–11** and **13**) were isolated from coral-derived fungus *Penicillium sclerotiorin*. Anti-inflammatory assay suggested that compounds **2**, **6** and **7** exhibited potential activity with the possible mechanism of downregulating the expression of iNOS and COX-2 in mRNA level. This study will make a contribution to the chemical diversities of polyketides especially the azaphilone derivatives and the discovery of potential anti-inflammatory agent from marine fungi.

Acknowledgement

We thank the National Natural Science Foundation of China (81741162, 21472251), the key project of Natural Science Foundation of Guangdong Province (2016A040403091) and the Special Promotion Program for Guangdong Provincial Ocean and Fishery Technology (A201701C06) for generous support.

Appendix A. Supplementary material

Supplementary data to this article can be found online at https://doi.org/10.1016/j.bioorg.2019.102973.

References

[1] J.W. Blunt, B.R. Copp, R.A. Keyzers, M.H.G. Munro, M.R. Prinsep, Marine natural products, Nat. Prod. Rep. 33 (2016) 382–431, https://doi.org/10.1039/c5np00156k.
[2] J.W. Blunt, B.R. Copp, R.A. Keyzers, M.H.G. Munro, M.R. Prinsep, Marine natural products, Nat. Prod. Rep. 34 (2017) 235–294, https://doi.org/10.1039/c6np00124f.
[3] Nat. Prod. Rep. 35 (1) (2018) 8–53, https://doi.org/10.1039/C7NP00052A.
[4] C. Nastrucci, A. Cesario, P. Russo, Anticancer drug discovery from the marine environment, Rec. Pat. Anti-canc. 7 (2012) 218–232, https://doi.org/10.2174/157489212799972963.
[5] T.F. Molinski, D.S. Dalisay, S.L. Lievens, J.P. Saludes, Drug development from marine natural products. Nat. Rev. Drug Disco. 8 (2009) 69 − 85. https://doi.org/10.1038 /nrd2487.
[6] X. Huang, H. Huang, H. Li, X. Sun, H. Huang, Y. Lu, Y. Lin, Y. Long, Z. She. Asperterpenoid A, a new sesterterpenoid as an inhibitor of mycobacterium tuberculosi s protein tyrosine phosphatase B from the culture of Aspergillus sp. 16-5c. Org. Lett. 15 (2013) 721 − 723. https://doi.org/10.1021/ol303549c.
[7] H. Cui, Y. Lin, M. Luo, Y. Lu, X. Huang, Z. She, Diaporisoindoles A-C: three isoprenylisoindole alkaloid derivatives from the mangrove endophytic fungus *Diaporthe* sp. SYSU-HQ3, Org. Lett. 19 (2017) 5621–5624, https://doi.org/10.1021/acs.orglett.7b02748.
[8] W.H. Jiao, B.H. Cheng, G.D. Chen, G.H. Shi, J. Li, T.Y. Hu, H.W. Lin, Dysiarenone, a dimeric C21 meroterpenoid with inhibition of COX-2 expression from the marine sponge *Dysidea arenaria*, Org. Lett. 20 (2018) 3092–3095, https://doi.org/10.1021/acs.orglett.8b01148.
[9] H.L. Li, R. Xu, X.M. Li, S.Q. Yang, L.H. Meng, B.G. Wang, Simpterpenoid A, a meroterpenoid with a highly functionalized cyclohexadiene moiety featuring gem-Propane-1, 2-dione and methylformate groups, from the mangrove-derived Penicillium simplicissimum MA-332. Org. Lett. 20 (2018) 1465 − 1468. https://doi.org/10.1021/acs.orglett.8b00327.
[10] Z. Liu, G. Xia, S. Chen, Y. Liu, H. Li, Z. She, Eurothiocin A and B, sulfur-containing benzofurans from a soft coral-derived fungus Eurotium rubrum SH-823. Mar. Drugs. 12 (2014) 3669 − 3680. https://doi.org/10.3390/md12063669.
[11] C.J. Zheng, C.L. Shao, Z.Y. Guo, J.F. Chen, D.S. Deng, K.L. Yang, Y. Chen, X.M. Fu, Z.G. She, Y.C. Lin, C.Y. Wang, Bioactive hydroanthraquinones and anthraquinone dimers from a soft coral-derived *Alternaria* sp Fungus, J. Nat. Prod. 75 (2012) 189–197, https://doi.org/10.1021/np200766d.
[12] C.L. Shao, H.X. Wu, C.Y. Wang, Q.A. Liu, Y. Xu, M.Y. Wei, P.Y. Qian, Y.C. Gu, C.J. Zheng, Z.G. She, Y.C. Lin, Potent antifouling resorcylic acid lactones from the gorgonian-derived fungus *Cochliobolus lunatus*, J. Nat. Prod. 74 (2011) 629–633, https://doi.org/10.1021/np100641b.
[13] S. Liu, M. Su, S. Song, J. Hong, H.Y. Chung, J.H. Jung, An anti-Inflammatory PPAR-γ agonist from the jellyfish-Derived fungus *Penicillium chrysogenum* J08NF-4, J. Nat. Prod. 81 (2018) 356–363, https://doi.org/10.1021/acs.jnatprod.7b00846.
[14] M.J. Frisch, G.W. Trucks, H.B. Schlegel, et al. Gaussian 09, revision D.01, Gaussian, Inc., Wallingford, CT, 2013.
[15] G.M. Morris, R. Huey, W. Lindstrom, M.F. Sanner, R.K. Belew, D.S. Goodsell, A.J. Ollson, Autodock4 and AutoDockTools4: automated docking with selective receptor flexibility, J. Comput. Chem. 16 (2009) 2785 − 363. https://doi.org/10.1002/jcc.21256.
[16] Z. Liu S. Chen P. Qiu C. Tan Y. Long Y. Lu Z. She, (+)- and (−)-Ascomlactone A: a pair of novel dimeric polyketides from a mangrove endophytic fungus Ascomycota sp. SK2YWS-L, Org. Biomol. Chem. 15, (2017) 10276 − 10280. https://doi.org/ 10.1039/C7OB02707A.
[17] K. Matsuzaki, H. Ikeda, R. Masuma, H. Tanaka, S. Omura, Isochromophilones I and II, novel inhibitors against gp120-CD4 binding produced by *Penidllium multicolor* FO-2338, J. Antibiot. 48 (1995) 496–806, https://doi.org/10.7164/antibiotics.48.703.
[18] R.A. Eade, H. Page, A. Robertson, K. Turner, W.B. Whalley, The chemistry of fungi. Part XXVIII. Sclerotiorin and its hydrogenation products, J. Chem. Soc. (Resumed) (1957) 4913–4924, https://doi.org/10.1039/JR9570004913.
[19] N. Arai, K. Shiomi, H. Tomoda, N. Tabata, D.J. Yang, R. Masuma, T. Kawakubo, S. Omura, Isochromophilones III-VI, inhibitors of acyl-CoA: cholesterol acyltransferase produced by *Penicillium multicolor* FO-3216, J. Antibiot. 48 (1995) 696–702, https://doi.org/10.7164/antibiotics.48.696.
[20] K. Matsuzaki, H. Tahara, J. Inokoshi, H. Tanaka, New brominated and halogen-less derivatives and structure-activity relationship of azaphilones inhibiting gp120-CD4 binding, J. Antibiot. 51 (1998) 1004–1011, https://doi.org/10.7164/antibiotics.51.1004.
[21] A.P. Michael, E.J. Grace, M. Kotiw, R.A. Barrow, Isochromophilone IX, a novel GABA-containing metabolite isolated from a cultured fungus *Penicillium* sp, Aust. J. Chem. 56 (2003) 13–15, https://doi.org/10.1071/CH02021.
[22] J. Li, X. Yang, Y. Lin, J. Yuan, Y. Lu, X. Zhu, et al., Meroterpenes and azaphilones from marine mangrove endophytic fungus *Penicillium* 303, Fitoterapia 97 (2014) 241–246, https://doi.org/10.1016/j.fitote.2014.06.011.
[23] A.A. Stierle, D.B. Stierle, T. Bugni, Sequoiatones A and B: novel antitumor metabolites isolated from a redwood endophyte, J. Org. Chem. 64 (1999) 5497–15484, https://doi.org/10.1021/jo990277l.
[24] W.S. Borges, G. Mancilla, D.O. Guimaraes, R. Duran-Patron, I.G. Collado, M.T. Puto, Azaphilones from the dndophyte *Chaetomium globosum*, J. Nat. Prod. 74 (2011) 1182–1187, https://doi.org/10.1021/np200110f.
[25] W. Chen, R. Chen, Q. Liu, Y. He, K. He, X. Ding, L. Kang, X. Guo, N. Xie, Y. Zhou, Y. Lu, R.J. Cox, I. Molnar, M. Li, Y. Shao, F. Chen, Orange, red, yellow: biosynthesis of azaphilone pigments in *Monascus* fungi, Chem. Sci. 8 (2017) 4917–4925, https://doi.org/10.1039/C7SC00475C.
[26] A.D. Somoza, K.H. Lee, Y.M. Chiang, B.R. Oakley, C.C.C. Wang, Reengineering an azaphilone biosynthesis pathway in *Aspergillus nidulans* to create lipoxygenase inhibitors, Org. Lett. 14 (2012) 972–975, https://doi.org/10.1021/ol203094k.